Published in Applied Physics Letters 71, 3200-3202, 1997
which should be used for any reference to this work

Characterization of intra-cavity reflections by Fourier transforming spectral data of optically pumped InGaN lasers

Daniel Hofstetter,[a] Linda T. Romano, Robert L. Thornton, David P. Bour, and N. M. Johnson
Xerox Palo Alto Research Center, Palo Alto, California 94304

Fourier analysis of laser emission spectra just above threshold is used to evaluate the impact of structural defects on the emission from optically pumped InGaN lasers. By dry etching a 300-nm-deep groove into the surface of a laser bar, we have modified the emission spectrum of such a device in a controlled manner. The occurrence of sharp features in the Fourier transformed spectrum allowed the identification of the mode spacing corresponding to the full cavity length, as well as to fractions of the full cavity length due to the etched groove. This enables us to identify additional features in the transform spectrum as being due to scattering centers within the waveguide. Identification of the density and strength of such centers is an important capability for the fabrication of blue diode lasers in the gallium–nitride material system.

The development of a blue laser diode in the gallium–nitride material system has attracted considerable attention because of its potential impact on high resolution scanners and printers and high storage density optical disks.[1–3] One major problem of the nitrides is their large lattice mismatch to available substrates. This mismatch causes the material to crack or to form edge dislocations, leading to severe scattering loss within the laser cavity.[4] However, it is difficult to evaluate the impact of crystal imperfections on the reflection and scattering loss in the optical cavity. The most common method, transmission electron microscopy (TEM), involves time-consuming sample preparation by ion milling or polishing.[5,6] It can confirm that there are cracks or pits in the material, but reveals little information about their spatial distribution along the laser cavity. Surface pits, as will be shown below, can be detected by using an atomic force microscope (AFM), but supplementary techniques are needed to determine their depth and the extent to which these impinge on the lasing cavity.

We report in this letter a new method to determine the presence of cracks and pits in a laser cavity. The way we address this issue is to look at the spectral signature of the imperfections by investigating the Fourier transform of the laser emission spectrum obtained under optical pumping conditions.[7–10] This approach requires neither the tedious processing which is necessary to fabricate an electrically pumped device such as a light emitting diode or a laser diode nor the effort to prepare a TEM sample. Nevertheless, it reveals some very important features of the quality of the optical waveguide, and is therefore expected to become a suitable diagnostic tool for improving device performance.

The experimental setup was very similar to our earlier experiments.[7] Since the emission of our optically pumped InGaN-based lasers exhibited two main emission lobes at angles of $\pm 18°$, we collected the light with a microscope objective (magnification 50×, numerical aperture 0.95) and focused it onto a quartz fiber with which we could feed it into a high resolution grating spectrometer (SPEX, $d_{\text{focus}} = 1.26$ m, $\Lambda = 1800$ lines/mm, $w_{\text{slit}} = 50$ μm). Signals were measured by a 1024 element array photodetector. The illumination time was on the order of 30 s in order to achieve good signal to noise ratios. Using this configuration, we achieved a spectral resolution of 0.25 Å over a wavelength window of 10 nm.

For these experiments, we used metalorganic chemical vapor deposition (MOCVD) grown samples with a 4-μm-thick GaN buffer, a 500 nm AlGaN lower clad, a 240 nm GaN waveguide with 5 InGaN quantum wells (QWs), and a 50-nm-thick upper clad on top. We investigated both samples where cracks were visible and samples in which we did not expect cracks. The 510-μm-long laser cavities were formed by two polished facets and a high reflectivity (HR) Al mirror on one side ($R = 93\%$). As shown in Fig. 1, a 5-μm-wide and 300-nm-deep groove was dry etched into a sample that we did not expect to be cracked. The etched groove was oriented at a shallow angle to the emitting facets, and divided the main cavity into two shorter sub cavities of variable length. At position A, there is no etched groove. At position B, the two sub cavities were 200 and 310 μm long, respectively. At position C, they measure 240 and 270 μm.

Fourier transforms of the laser spectra of the devices at positions A, B, and C allowed us to compare the effect of the etched groove and the crystal imperfections on the laser spectrum.[11,12] Obviously, the etched groove and those re-

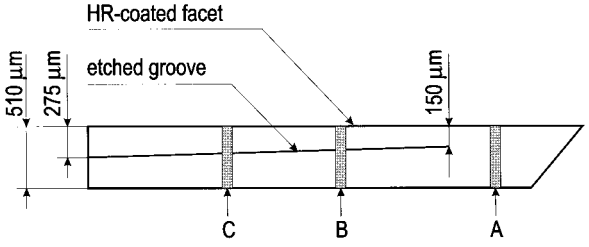

FIG. 1. Schematic top view of the device under investigation. The positions where spectra have been measured are marked with A, B, and C.

[a]Electronic mail: hofstetter@parc.xerox.com

flecting features which give sufficient backscattering into the waveguide mode serve as additional, parasitic mirrors within the laser cavity. Each additional reflection forms its own two Fabry-Pérot (FP) sub cavities; one with the back and one with the front facet. If there is more than one intra-cavity reflection, then there are even more possibilities for the formation of sub cavities. Let us assume here for simplicity that each feature produces only one pair of sub cavities. We therefore expect each of these sub cavities to have its own Fabry-Pérot mode spacing, corresponding to one peak pair in the Fourier transform of the emission spectrum.

In order to show the principle, we use a simple mathematical example. We start with a laser spectrum having a Gaussian-shaped envelope and cosinelike FP mode oscillations with mode spacing $\Delta\beta$, defined by

$$\Delta\beta = \frac{\pi}{nL}. \tag{1}$$

Although $\Delta\beta$ is in fact—via the dispersion correction—a function of the wave number, we assume here for simplicity a constant refractive index over the small wave number range we are investigating. The spectrum of such a device is then given by

$$f(\beta) = e^{-\pi\left(\frac{\beta_0-\beta}{w}\right)^2} \cdot \left[1 + m \cdot \cos\left(\frac{2\pi^2\beta}{\Delta\beta \cdot n}\right)\right]. \tag{2}$$

In Eq. (1), L defines the cavity length and n is the dispersion-corrected effective refractive index, assumed to be constant. In Eq. (2), we define w as the full width at half maximum (FWHM) of the spectral envelope, and m as the contrast of the FP mode fringes. With β (wave numbers) and d (optical path length) as conjugate transform variables, the Fourier transformation of the above spectrum is defined by

$$\begin{aligned} F(d) &= \int_{-\infty}^{+\infty} f(\beta) \cdot e^{-2\pi i\beta d} d\beta \\ &= C_1 \cdot \left[e^{-\pi(wd)^2} + \frac{m}{2} \cdot \left(e^{-\pi\left(w \cdot \left[d - \frac{\pi}{\Delta\beta \cdot n}\right]\right)^2} - \right.\right. \\ &\quad \left.\left. + e^{-\pi\left(w \cdot \left[d + \frac{\pi}{\Delta\beta \cdot n}\right]\right)^2} \right) \right] \end{aligned} \tag{3}$$

with C_1 being a complex constant. Since, in this particular case, $F(d)$ is an even function of d $[F(d) = F(-d)]$, we investigate only the peaks on the positive x axis. If we start with a device with an intra-cavity reflection defining two different sub-cavity lengths, $L = L_1 + L_2$, then these three different cavity lengths, L, L_1, and L_2, will initiate three different FP mode spacings, $\Delta\beta$, $\Delta\beta_1$, and $\Delta\beta_2$, respectively. The three corresponding cosine functions added together yield the spectrum of this device, where the sum of their Fourier transforms results in the transform of the spectrum. We will therefore end up with two Gaussian-shaped peaks at $d_0 = 0$ and at $d = \pi/(\Delta\beta \cdot n)$ and two additional peaks at $d_1 = \pi/(\Delta\beta_1 \cdot n)$ and at $d_2 = \pi/(\Delta\beta_2 \cdot n)$. Since we assumed $L = L_1 + L_2$, it follows that $d = d_1 + d_2$. Although these transforms are in general complex functions, we will present here the amplitude function only and hide the phase; this is appropriate because the amplitude contains the important information.

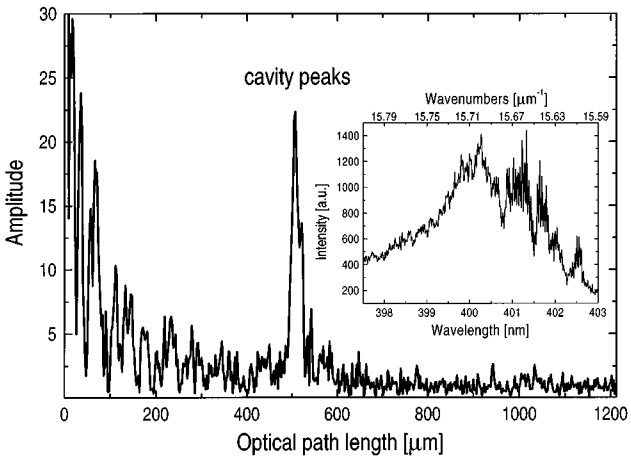

FIG. 2. Fourier transformed emission spectrum of the laser measured at position A. The spectrum, which is shown as an inset, was measured with a high resolution spectrometer.

We measured the emission spectra of the sample shown in Fig. 1 at a position beyond the etched groove (position A), and at two further positions within the grooved region (positions B and C). These positions are also shown in Fig. 1. Figure 2 shows the Fourier transformed emission spectrum of the unperturbed laser cavity at position A and, as an inset, the emission spectrum itself. There are clearly visible Fabry-Pérot oscillations in the spectrum which give rise to very pronounced cavity length peaks at around 510 μm in the transform. The origin of this peak family instead of a single peak is a result of filamenting in the laser cavity: since the films were grown without rotation of the sapphire substrate, there is a substantial thickness gradient across the wafer. The fact that we see a Gaussian far field distribution with a FWHM of 7° perpendicular to the growth direction allows us to estimate the lateral aperture width to be approximately 25 μm. However, we estimate that the width of the pumped region is over 100 μm. Assuming therefore that there are several lasing filaments across the pumped area and considering the thickness gradient in the layers, we can expect multiple emission wavelengths and therefore more than one cavity length peak in the Fourier transform of the spectrum. There are many other features in the transform spectrum with optical path lengths below 510 μm. This structure must be due to additional perturbations within the laser cavity. We have seen data for which the inverse mode separations of pairs of these additional peaks add up to the mode spacing of the full cavity length peak, as described above. This implies the presence of discrete scattering centers at specific locations within the cavity. The fine structure of this transformed spectrum is in sharp contrast to what we observe in a laser cavity known to be free of optical perturbations, for example, the one from a red InGaAlP laser. The transformed spectrum of such a device is structureless except for the single peak due to the Fabry-Pérot modes.

A measurement of the emission spectra at positions B and C resulted typically in Fourier transforms as shown in Fig. 3. Both of them revealed peak pairs whose inverse spacings were clearly related to the distance to the grooved facet for each particular position. This establishes that the etched

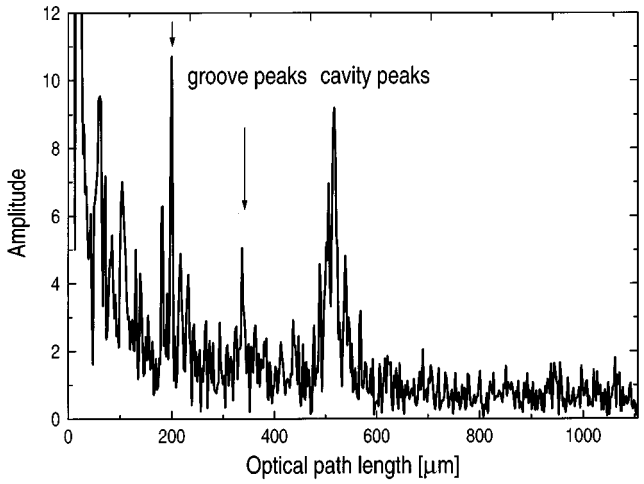

FIG. 3. Fourier transformed spectrum taken at position B. The peak pair corresponding to the etched groove is marked by arrows.

groove adds additional peaks to the transform of the existing laser spectrum, at positions determined by the position of the etched groove within the cavity. This peak structure is not noise. In addition, there are numerous additional peaks of similar height in the Fourier transform caused by different types of crystal imperfections. These peaks are also not noise. If we estimate an approximate number of $n_p = 50-100$ peaks to be present in the transformed spectrum and all of them caused by mutually interacting scattering centers, then we can calculate their number, n_s, by using

$$n_p = \sum_{k=1}^{n_s} k = \frac{n_s(n_s+1)}{2}. \tag{4}$$

From this equation, we get a number of $n_s = 10-15$ scatterers (corresponding to 30–50 μm distance between them) to be present in our sample.

In heavily cracked samples, the cracks are found to form on the prism planes. For this sample, we investigated ~ 50 μm of material in the TEM; by tilting the sample $\pm 30°$ in the microscope, we looked for cracks along four of the six prism planes. However, no cracks were observed, excluding them as a possible source of internal reflection.

Rather than cracks, the TEM investigation of this sample [Fig. 4(a)] revealed hexagonally shaped, 300-nm-deep and 250-nm-wide pits that extended from the surface into the active layer. By doing an AFM surface scan [Fig. 4(b)], we found an average pit-to-pit distance of 2 μm. This figure, taken by itself, is higher than the density of scatterers given by the number of reflection peaks. However, it is likely that the laser filaments are established along lines which minimize scattering loss and therefore minimize the number of pit intersections. In addition, it is possible that some number of pits do not backscatter into the waveguide mode. It is clear, however, that the extensive fine structure in the Fourier transform emission spectrum is a direct consequence of the pits present in the growth surface.

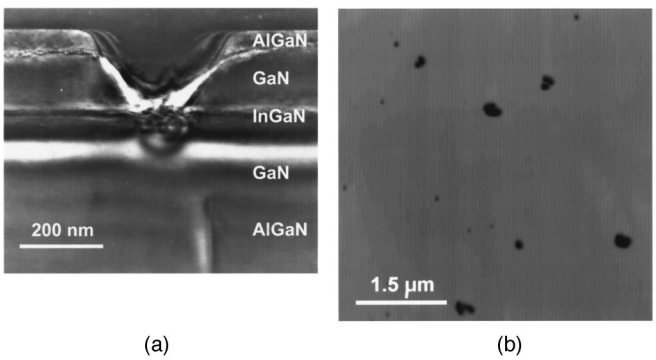

FIG. 4. TEM micrograph (120 000×)/AFM surface scan (6×6 μm^2) of a piece of the material from which the investigated sample was fabricated. The largest pits are hexagonally shaped, measure 250 nm across, and are 300 nm deep.

In summary, we have shown a new, powerful method for the investigation of the material quality of InGaN-based laser material. The method is based on Fourier transforming the spectral data of optically pumped laser devices. The main scattering features within the laser cavity of our material appeared to be pits in the surface which penetrate to the active region. Since the laser oscillates in narrow filaments, even relatively small pits can cause a strong back reflection resulting in the insertion of fine structure into the Fourier transformed spectrum. These features are introduced as pairs, and the optical path lengths of such a pair add up to the optical path length of the full cavity length peak. Since our method requires only simple processing, it offers an important diagnostic technique for the evaluation of the structural integrity of the optical waveguide.

The authors are grateful to F. Endicott, D. F. Fork, and G. Anderson for setting up the experiment. This work was financially supported by the United States Department of Commerce (DoC Contract No. ATP-70NANB2H1241, and the Defense Advanced Research Projects Agency (DARPA Contract No. MDA972-95-3-008).

[1] S. Nakamura, M. Senoh, S. Nagahama, N. Iwasa, T. Yamada, T. Matsushita, H. Kiyoku, and Y. Sugimoto, Jpn. J. Appl. Phys., Part 1 **35**, L74 (1996).
[2] S. Nakamura, M. Senoh, S. Nagahama, N. Iwasa, T. Yamada, T. Matsushita, Y. Sugimoto, and H. Kiyoku, Appl. Phys. Lett. **69**, 1477 (1996).
[3] D. P. Bour, H. F. Chung, W. Götz, L. Romano, B. S. Krusor, F. A. Ponce, N. M. Johnson, and R. D. Bringans, Electrochem. Soc. Proc. **96–11**, 37 (1996).
[4] Z. L. Liau, R. L. Aggarwal, P. A. Maki, R. J. Molnar, J. N. Walpole, R. C. Williamson, and I. Melngailis, Appl. Phys. Lett. **69**, 1665 (1996).
[5] L. T. Romano, B. S. Krusor, W. Götz, N. M. Johnson, R. J. Molnar, and E. Brown, Mater. Res. Soc. Symp. Proc. **433**, (1996).
[6] F. A. Ponce, B. S. Krusor, J. S. Major, Jr., W. E. Plano, and D. F. Welch, Appl. Phys. Lett. **67**, 410 (1995).
[7] D. Hofstetter, D. P. Bour, R. L. Thornton, and N. M. Johnson, Appl. Phys. Lett. **70**, 1650 (1997).
[8] H. Amano, T. Asahi, and I. Akasaki, Jpn. J. Appl. Phys., Part 1 **29**, L205 (1990).
[9] T. J. Schmidt, X. H. Yang, W. Shan, J. J. Song, A. Salvador, W. Kim, Ö. Aktas, A. Botchkarev, and H. Morkoç, Appl. Phys. Lett. **68**, 1820 (1996).
[10] A. S. Zubrilov, V. I. Nikolaev, V. A. Dmitriev, K. G. Irvine, J. A. Edmond, and C. H. Carter, Jr., Inst. Phys. Conf. Ser. **141**, 525 (1994).
[11] B. D. Patterson, C. Musil, H. Siegwart, and A. Vonlanthen, Microelectron. Eng. **27**, 347 (1995).
[12] B. D. Patterson, J. E. Epler, B. Graf, H. W. Lehmann, and H. C. Sigg, J. Quantum Electron. **J-QE 30**, 703 (1994).